J Fluoresc (2010) 20:551–556
DOI 10.1007/s10895-009-0579-3

ORIGINAL PAPER

Study on the Intracellular Fate of Tat Peptide-Conjugated Quantum Dots by Spectroscopic Investigation

Rongling Xiong · Zheng Li · Lan Mi · Pei-Nan Wang · Ji-Yao Chen · Lixin Wang · Wu-Li Yang

Received: 9 September 2009 / Accepted: 7 December 2009 / Published online: 19 January 2010

Abstract The photoluminescence (PL) spectrum of water-soluble thiol-capped CdTe quantum dots (QDs) conjugated with Tat peptide in solution showed a remarkable redshift as compared to that of unconjugated QDs. After cellular uptake of the Tat-QDs conjugates, the micro-PL spectrum of Tat-QDs in lysosomes showed a spectral blueshift, which was most probably due to the fact that Tat peptide was digested by the enzymes, leaving the Tat-detached QDs in lysosomes. The reasons for the spectral changes have been discussed in detail.

Keywords Quantum dots · Tat peptide-conjugated · Micro-PL spectrum · Living cells

Introduction

Water-soluble semiconductor colloidal quantum dots (QDs), such as CdSe and CdTe QDs, have attracted increasing worldwide attentions as a new class of fluorescent probes. Compared to traditional organic dyes and fluorescent proteins, QDs have advantages in cellular labeling, such as high photoluminescence (PL) efficiency, broad excitation with narrow emission bands, and resistance to photobleaching. Moreover, the emission spectra of QDs can be tuned from the ultraviolet to the infrared by simply changing their sizes [1, 2]. This unique optical property makes them possible for multiplex labeling with a single excitation source [3, 4]. The cytotoxicities of CdSe and CdTe QDs, which are mainly caused by the release of free cadmium ions, have been studied by previous works [5–7]. With appropriate surface coatings, a low concentration in use and minimizing the illumination, the cytotoxicity of QDs can be effectively reduced.

In the recent years, more and more investigations have been focused on the applications of QDs that are functionalized by conjugating to diverse ligands for different purposes [8–11]. For example, peptides are widely used as the bridges between QDs and their cargos [12, 13]. Tat peptide, derived from the HIV-1 Tat protein, belongs to the family of cell-penetrating peptides (CPPs) [14]. Because of its abundance of positively charged amino acids, lysine (Lys, K) and arginine (Arg, R), it is easy for Tat peptide to bind to the negatively charged plasma membranes to facilitate cellular uptake [15]. Tat peptide was reported as a cellular delivery vector for biological macromolecules, such as proteins, DNA and liposomes [15, 16]. When conjugating to QDs, it can enhance the cellular uptake efficiency of QDs [17–19]. Tat peptide may also be used as a novel bridge between QDs and their cargos by further binding the cargos to Tat peptide-conjugated QDs (Tat-QDs) at the C terminus of Tat peptide. The cargo-Tat-QD conjugates, which have the advantages of both QDs and Tat peptide, might have a bright future for drug delivery.

When QDs were conjugated with Tat peptide, spectral shifts of PL were observed. However, there exist diverse explanations for the mechanism of the spectral changes. Wang et al. [20–22] thought that the reason lies in the

R. Xiong · Z. Li · L. Mi (✉) · P.-N. Wang
Department of Optical Science and Engineering,
Fudan University,
Shanghai 200433, China
e-mail: lanmi@fudan.edu.cn

J.-Y. Chen
Surface Physics Laboratory (National key laboratory),
Department of Physics, Fudan University,
Shanghai 200433, China

L. Wang · W.-L. Yang
Department of Macromolecular Science and Key Laboratory
of Molecular Engineering of Polymers, Fudan University,
Shanghai 200433, China

increased final sizes of QDs when they covalently attached to human IgG, transferrin (Tf) or mouse anti-human CD71 monoclonal antibody. Whereas, Dif et al. [23] attributed the redshift to the change of the electronic structure of the QD surface after conjugated to a peptide with the sequence of -CCCSSSD-. Dwarakanath et al. [24] and Gao et al. [25] supposed that pH had an effect on the PL spectra of QDs. However, Anandampillai et al. [26] presented a computational 19 nm redshift in the emission peak of the CdSe QDs (1.1 nm) upon interaction with a DNA molecule, which gave a set of torsions to the QD structure. In the present work, Tat-QDs were synthesized and used to label living cells. Their optical properties in living cells were studied in detail.

Materials and methods

Preparation of Tat-QDs

The water-soluble thiol-capped CdTe QDs were synthesized using a method reported previously [27] with a slight change in the molar ratio of the reactants. The sequence of Tat peptide (Shanghai Science Peptide Biological Technology Co., Ltd.) is -RKKRRQRRR-. The Tat-QDs were prepared in a method reported by previous works [28, 29] by stirring the solution containing QDs with Tat peptide at a ratio of 1:1 for 36 h at room temperature. During the preparation of Tat-QDs, the pH value was adjusted to 8.5 in order to prevent the aggregation of QDs. After the reaction, the solution was centrifuged at a speed of 15,000 rpm for 1 h to remove the aggregated QDs. The supernatant was used for experiments. Since each QD has about thousands of 3-mercaptoacetic acid (MPA) molecules on its surface, the amount of which was much larger than that of Tat peptide in the solution. It was almost impossible that free Tat peptide would be left unconjugated to the QDs.

Cell staining

Human hepatocellular carcinoma (QGY) cells were seeded onto culture dishes containing DMEM-H medium with 10% calf serum and were cultured in a humidified incubator (37 °C and 5% CO_2) for 24 h to reach 80% confluence with normal morphology. The Tat-QDs aqueous solution was then added into the growth medium to achieve a final concentration of 600 nM. The cells were incubated for 2 h and then washed with DMEM-H medium for 3 times. During the spectral measurement, the cells were kept at 37 °C in a temperature controller. LysoTracker Green DND-26 (LysoTracker), bought from Invitrogen (Molecular Probes) Corporation, was used as the indicator of lysosomes. LysoTracker was added in the growth medium at the concentration of 50 nM for 5 min to stain lysosomes and then the cells were washed with DMEM-H medium for 3 times. The absorption maximum of the indicator is at 504 nm and the fluorescence emission peak at 511 nm.

Measurements of micro-PL spectra in living cells

The fluorescence images of the intracellular distributions of QDs and lysosomes were measured with a laser scanning confocal microscope (LSCM) (Olympus, FV-300, IX71), using a 488 nm CW Ar^+ laser (Melles Griot) as the excitation source. The laser beam was focused by a 60× oil objective to a spot of about 1 μm in diameter. The images of QDs and lysosomes were recorded simultaneously in two channels of the microscope with a 585–640 nm bandpass filter for QDs and a 505–550 nm bandpass filter for lysosomes. The three-dimensional distributions of QDs and lysosomes in a cell were obtained by using the z-scan mode. On the basis of the obtained micrographs, we selected some spots in a cell to measure the micro-PL spectra using the point-scan mode of the microscope. After the image was acquired, the Ar^+ excitation laser was switched to a 405 nm semiconductor laser (Coherent) to measure the spectra, which was aligned collinear with the beam from the Ar^+ laser before the micrograph of the cell was measured. In this case, the PL spectra at the selected point could be measured exactly. The PL output from the side exit of the microscope was directly focused onto the entrance slit of the spectrometer. The PL spectra were recorded with a spectrometer (Acton, Spectro-pro 2150i) equipped with a liquid-nitrogen-cooled CCD (Princeton, Spec-10:100B LN).

Measurements of PL spectra for solutions

A series of cell-free spectral measurements was conducted to detect the spectral changes after diverse reagents were added to the QD solutions. The reagents included PEG (polyethylene glycol, 3,350 Da, Sigma), BSA (bovine serum albumin, 68 kDa, Sigma), dextran (70 kDa, Sigma-Aldrich), Histone (Calf Thymus H) (15 kDa, Worthington), and Casein (23.6 kDa, Worthington). The solutions were set in a 96-hole dish and the PL spectra were measured with the LSCM similarly to that for living cells. The laser beam was focus by a 20× objective to achieve a larger illumination spot in the solutions.

Results and discussion

Mechanism of the spectral redshift of Tat-QDs in aqueous solution

The PL spectra of unconjugated QDs (without reaction with Tat peptide) and Tat-QDs in solutions are showed in Fig. 1.

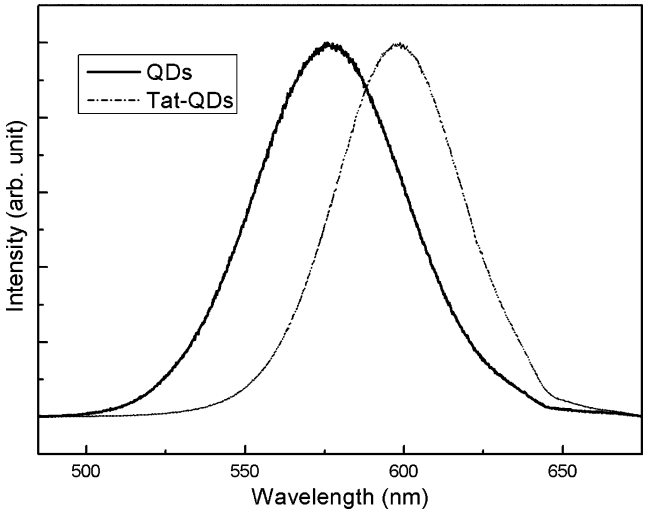

Fig. 1 The PL spectra of QDs and Tat-QDs in aqueous solutions

A spectral redshift from 576 nm of unconjugated QDs to 597 nm of Tat-QDs is observed. The redshift must be due to the conjugation of Tat peptide with the MPA at the QD surface.

As mentioned in the introduction section, different explanations were brought forward for the spectral redshift of Tat-QDs. It is well known that the emission wavelength of QDs is dominantly dependent on the size of the semiconductor core. Therefore, the increase of the final size of QDs by conjugation with Tat peptide could not cause such a large redshift of 21 nm in our experiment. The pH effect on the PL redshift was also suggested [24]. To test the pH effect, we gradually changed the pH value from 8.5 to 2 by adding a diluted H_2SO_4 solution after the Tat-QDs were produced. No significant spectral change was detected. Electrostatic interaction was another proposed reason [23]. Since the conjugations via electrostatic interaction are not sufficiently stable and can be easily disrupted by adding extra ions as a result of the counter-ion screening effect [30, 31], we added NaCl to a Tat-QDs solution to a concentration as high as 1 M to examine the electrostatic interactions. No spectral shift was observed (data not shown), indicating that the conjugation of Tat peptide with QDs could not result from the electrostatic binding. Considering the precursors in the reaction for producing Tat-QDs conjugates, the formation of hydrogen bonds is mostly expected. Since the molar ratio of QDs to Tat peptide was 1:1 in this work, there was only one Tat peptide conjugated to the surface of one QD on an average. The asymmetrically distributed hydrogen bonds could cause the deformation potential of QDs, which would change the energy band of QDs as reported previously [24, 26, 32]. Theoretically, an increase in the amount of Tat peptide bonded on QDs would bring about a more symmetrical distribution of Tat peptide around QDs and therefore reduce the effect of the deformation potential. However, a large amount of Tat peptide would lead to the aggregation of QDs. To test this supposition, L-Lysine (Lys, K, Sigma-Aldrich) and L-Arginine (Arg, R, Sigma-Aldrich), which are the two main amino acids of Tat peptide, were used to conjugate to QDs instead. After Lys (or Arg) was mixed in the QD solution at a molar ratio of 200:1 and kept stirring for 48 h at room temperature, the emission peak of QDs only shifted from 576 nm to 580 nm. While changing the molar ratio to 1:1, the emission peak shifted to 590 nm as shown in Fig. 2. These results support our speculation that the asymmetrical conjugation of Tat peptide with QDs by hydrogen bonding results in the introduction of deformation potential, leading to the narrowing of the energy gap of QDs, namely the spectral redshift.

Intracellular distributions of Tat-QDs and the spectral characteristics

The intracellular distributions of Tat-QDs were shown in Fig. 3, where (a) and (b) demonstrate the intracellular distributions of lysosomes (green) and Tat-QDs (red) in an X-Y plane, respectively, (c) shows the differential interference contrast (DIC) image to exhibit the cell morphology and (d) is a merged image of (a) (b) and (c). The yellow color in Fig. 3(d) represents the mixed fluorescence from LysoTracker and Tat-QDs, demonstrating the co-localization of Tat-QDs and lysosomes. The X-Z and Y-Z profiles shown at the bottom and the right side of Fig. 3(d) display the distributions of lysosomes and Tat-QDs at the cross sections along the marked lines in the main image. During our experiments (about 1 h), no obvious morphological changes of QGY cells caused by cytotoxicity of QDs was observed.

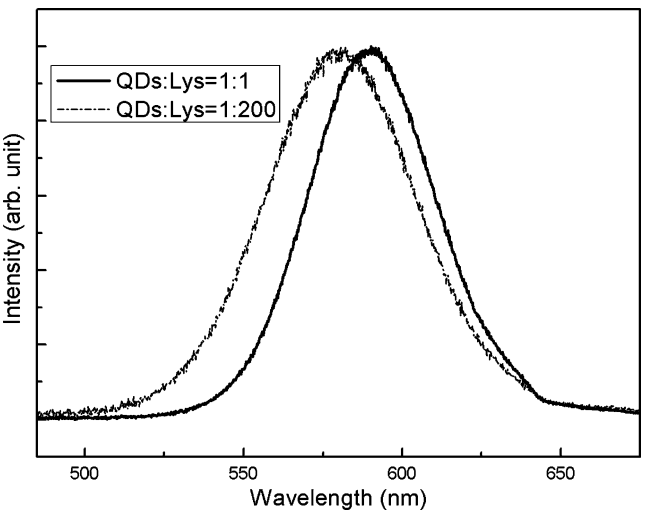

Fig. 2 The PL spectra of QDs solutions after adding Lys at the molar ratio of 1:200 and 1:1 respectively

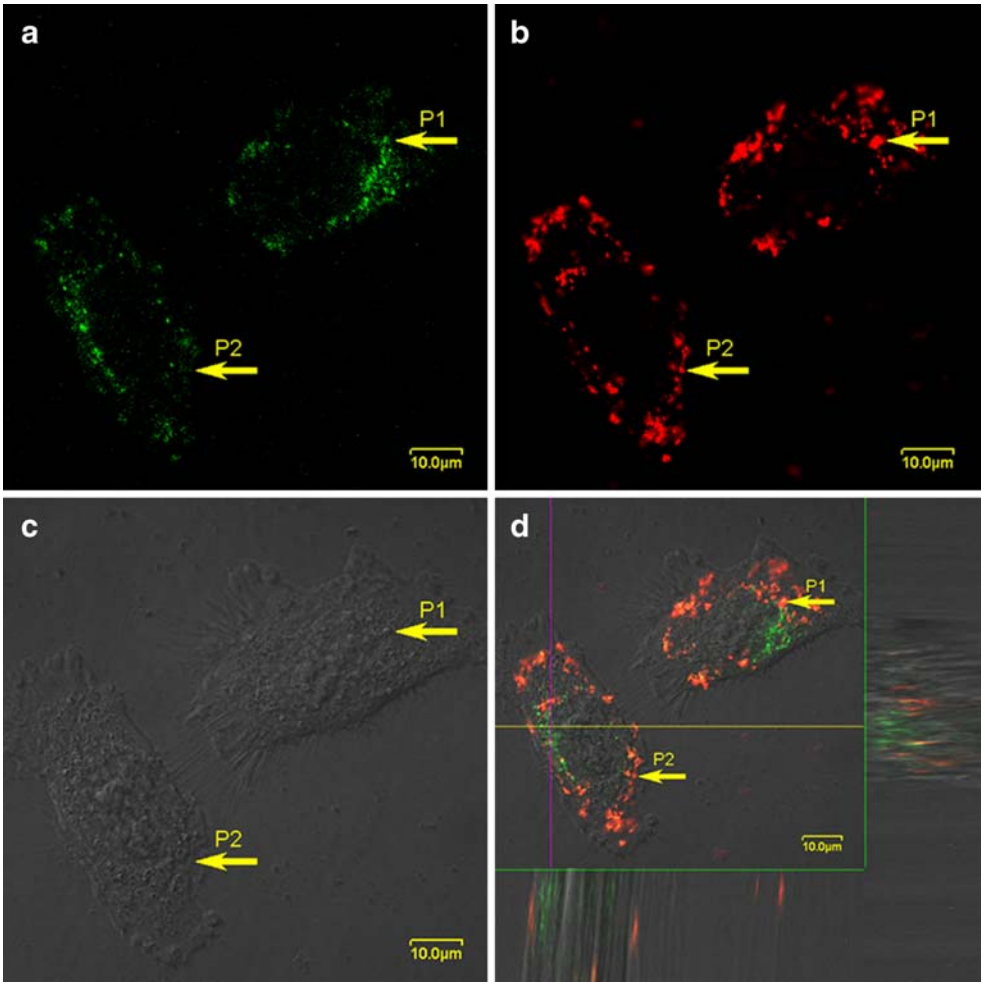

Fig. 3 Fluorescence images of the distribution of lysosomes and Tat-QDs in QGY cells. **a** The distribution of lysosomes; **b** the distribution of Tat-QDs; **c** DIC image of the cells; and (**d**) a merged image of **a** **b** and **c**. At the bottom and the right of (**d**) are the X-Z and Y-Z profiles measured along the lines marked in the main image, showing the three-dimensional distributions of Tat-QDs and lysosomes. *P1* is a spot in a lysosome and *P2* is far from any lysosome

Figure 4 displays two typical PL spectra of Tat-QDs in a QGY cell at P1 and P2 as marked in Fig. 3, where P1 is a spot just inside a lysosome and P2 is in the region far away from any lysosome. By measuring the PL spectra at several different spots inside and outside the lysosomes, the averaged wavelength at the PL peaks in lysosomes is 584 nm, while that far from any lysosome is 591 nm. The spectral difference is evident. Considering the primary function of lysosomes for hydrolyzing proteins to free amino acids, it was supposed that Tat peptide conjugated to QDs should be hydrolyzed by the digestive enzymes inside the lysosomes. Therefore, we incubated QGY cells with unconjugated QDs (without reaction with Tat peptide) and LysoTracker, using the same process as Tat-QD labeling. Similar to our previous results [33], the distributions of the unconjugated QDs in cytoplasm as well as in lysosomes

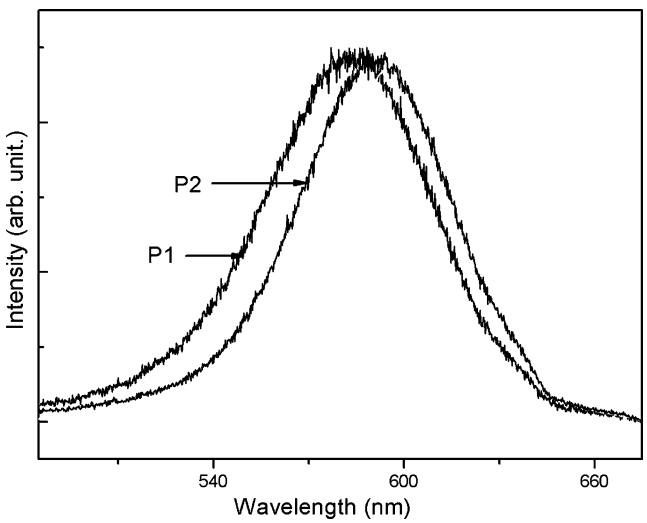

Fig. 4 The micro-PL spectra of Tat-QDs in QGY cells at P1 (*inside a lysosome*) and P2 (*outside lysosomes*) as marked in Fig. 3

Table 1 Averaged emission redshifts of unconjugated QD solutions after adding bio-agents

Agents	Redshifts (nm)
Histone (0.2 and 1 mM)	8 and 5
BSA (3 mM)	0
dextrans (2 mM)	13
PEG (60 mM)	13
Casein (0.2 mM)	6

were observed. By measuring their micro-PL spectra, their averaged emission peaks were at 584 nm (data not shown) either inside or outside the lysosomes, exactly the same as that of Tat-QDs in lysosomes. It means that Tat peptide was indeed digested by the enzymes, leaving Tat-detached QDs in lysosomes.

However, it should be noted that the emission peaks of the unconjugated QDs redshifted from 576 nm in aqueous solution to 584 nm in cells (either outside or inside the lysosomes). Considering the complex cellular environment, which is a crowded medium containing abundant macromolecules [34], the spectral shift is conceivable. To explore the influence of macromolecules, some bio-agents were added into the QD solutions respectively, and the resulted emission peaks are listed in Table 1. There were redshifts (5–13 nm) observed when QD solutions were mixed with Histone, Casein, dextrans and PEG, respectively, and no redshift was observed in the case of adding BSA (see Table 1). Therefore, some of the macromolecules do play a role in the spectral shift of water-soluble QDs although the mechanisms are not clear yet.

In the previous works, it was reported that Tat peptide was used to help cellular delivery of diverse cargos labeled with fluorescein for tracking [35–37]. Similarly, when QDs take the place of the fluorescein, cargo-Tat-QD conjugates have the benefit for both cargo delivery and tracking, which may have a bright future in drug delivery. After the conjugates reach their destination, the cargo may be easily released from the QDs through the digestion of Tat peptide, which could be traced and verified by the changes of the micro-PL of QDs. Walther et al. [13] supposed that the cargos of QDs were released at the site between peptide and cargos, while our work demonstrated that the site could be between the QDs and peptide instead. When the cargo is left in the cells for further functions, QDs must be excreted for human health. Nevertheless, the theoretical “blue print” is far from clinic applications. There are a lot of complicated problems to be solved, such as the methods of directing the cargo to its destination and egesting the cargo-detached QDs.

Conclusions

Conjugation of Tat peptide to QDs brought about the redshift of the PL spectrum, which is most probably due to the asymmetrical conjugation of Tat peptide with QDs. The microscopic fluorescence measurement shows that lysosome is one of the main destinations of Tat-QDs after cellular uptake. The spectroscopic study provides evidence that Tat peptide was digested in lysosomes and the Tat-detached QDs were left there. This may open a new way in the future for drug delivery.

Acknowledgements This work is supported by National Natural Science Foundation of China (10774027, 60638010) and Shanghai Educational Development Foundation (2008CG03).

References

1. Klostranec JM, Chan WCW (2006) Quantum dots in biological and biomedical research: recent progress and present challenges. Adv Mater 18:1953–1964
2. Resch-Genger U, Grabolle M, Cavaliere-Jaricot S, Nitschke R, Nann T (2008) Quantum dots versus organic dyes as fluorescent labels. Nat Methods 5(9):763–775
3. Parak WJ, Pellegrino T, Plank C (2005) Labelling of cells with quantum dots. Nanotechnology 16:R9–R25
4. Delehanty JB, Mattoussi H, Medintz IL (2009) Delivering quantum dots into cells: strategies, progress and remaining issues. Anal Bioanal Chem 393:1091–1105
5. Derfus AM, Chan WCW, Bhatia SN (2004) Probing the cytotoxicity of semiconductor quantum dots. Nano Lett 4(1):11–18
6. Hoshino A, Fujioka K, Oku T, Suga M, Sasaki YF, Ohta T, Yasuhara M, Suzuki K, Yamamoto K (2004) Physicochemical properties and cellular toxicity of nanocrystal quantum dots depend on their surface modification. Nano Lett 4(11):2163–2169
7. Lovrić J, Bazzi HS, Cuie Y, Fortin GRA, Winnik FM, Maysinger D (2005) Differences in subcellular distribution and toxicity of green and red emitting CdTe quantum dots. J Mol Med 83:377–385
8. Medintz IL, Uyeda HT, Goldman ER, Mattoussi H (2005) Quantum dot bioconjugates for imaging, labelling and sensing. Nat Mater 4:435–446
9. Hild WA, Breunig M, Goepferich A (2008) Quantum dots-Nano-sized probes for the exploration of cellular and intercellular targeting. Eur J Pharm Biopharm 68:153–168
10. Zhou M, Ghosh I (2006) Current trends in peptide science quantum dots and peptides: a bright future together. Biopolymers 88(3):325–339
11. Hoshino A, Fujioka K, Oku T, Nakamura S, Suga M, Yamaguchi Y, Suzuki K, Yasuhara M, Yamamoto K (2004) Quantum dots targeted to the assigned organelle in living cells. Microbiol Immunol 48:985–994
12. Medintz IL, Pons T, Trammell SA, Grimes AF, English DS, Blanco-Canosa JB, Dawson PE, Mattoussi H (2008) Interactions between redox complexes and semiconductor quantum dots coupled via a peptide bridge. J Am Chem Soc 130:16745–16756
13. Walther C, Meyer K, Rennert R, Neundorf I (2008) Quantum dot-carrier peptide conjugates suitable for imaging and delivery applications. Bioconjugate Chem 19:2346–2356
14. Lindgren M, Hällbrink M, Prochiantz A, Langel Ü (2000) Cell-penetrating peptides. Trends Pharmacol Sci 21:99–103
15. Kaplan IM, Wadia JS, Dowdy SF (2005) Cationic TAT peptide transduction domain enters cells by macropinocytosis. J Control Release 102:247–253
16. Brooks H, Lebleu B, Vives E (2005) Tat peptide-mediated cellular delivery: back to basics. Adv Drug Deliv Rev 57:559–577
17. Ruan G, Agrawal A, Marcus AI, Nie S (2007) Imaging and tracking of tat peptide-conjugated quantum dots in living cells: New insights into nanoparticle uptake, intracellular transport, and vesicle shedding. J Am Chem Soc 129:14759–14766
18. Lei Y, Tang H, Yao L, Yu R, Feng M, Zou B (2008) Applications of mesenchymal stem cells labeled with tat peptide conjugated quantum dots to cell tracking in mouse body. Bioconjugate Chem 19(2):421–427

19. Xue FL, Chen JY, Guo J, Wang CC, Yang WL, Wang PN, Lu DR (2007) Enhancement of intracellular delivery of CdTe quantum dots (QDs) to living cells by tat conjugation. J Fluoresc 17:149–154
20. Wang J-H, Liu T-C, Cao Y-C, Hua X-F, Wang H-Q, Zhang H-L, Li X-Q, Zhao Y-D (2007) Fluorescence resonance energy transfer between FITC and water-soluble CdSe/ZnS quantum dots. Colloids Surf A 302:168–173
21. Liu T-C, Wang J-H, Wang H-Q, Zhang H-L, Zhang Z-H, Hua X-F, Cao Y-C, Zhao Y-D, Luo Q-M (2007) Bioconjugate recognition molecules to quantum dots as tumor probes. J Biomed Mater Res A 83(4):1209–1216
22. Wang H-Q, Zhang H-L, Li X-Q, Wang J-H, Huang Z-L, Zhao Y-D (2008) Solubilization and bioconjugation of QDs and their application in cell imaging. J Biomed Mater Res A 86(3):833–841
23. Dif A, Henry E, Artzner F, Baudy-Floc'h M, Schmutz M, Dahan M, Marchi-Artzner V (2008) Interaction between water-soluble peptidic CdSe/ZnS nanocrystals and membranes: formation of hybrid vesicles and condensed lamellar phases. J Am Chem Soc 130(26):8289–8296
24. Dwarakanath S, Bruno JG, Shastry A, Phillips T, John A, Kumar A, Stephenson LD (2004) Quantum dot-antibody and aptamer conjugates shift fluorescence upon binding bacteria. Biochem Biophys Res Commun 325:739–743
25. Gao X, Chan WCW, Nie S (2002) Quantum-dot nanocrystals for ultrasensitive biological labeling and multicolor optical encoding. J Biomed Opt 7(4):532–537
26. Anandampillai S, Zhang X, Sharma P, Lynch GC, Franchek MA, Larin KV (2008) Quantum dot-DNA interaction: computational issues and preliminary insights on use of quantum dots as biosensors. Comput Method Appl Math 197:3378–3385
27. Guo J, Yang W, Wang C (2005) Systematic study of the photoluminescence dependence of thiol-capped CdTe nanocrystals on the reaction conditions. J Phys Chem B 109(37):17467–17473
28. Delehanty JB, Medintz IL, Pons T, Brunel FM, Dawson PE, Mattoussi H (2006) Self-assembled quantum dot-peptide bioconjugates for selective intracellular delivery. Bioconjugate Chem 17:920–927
29. Mattheakis LC, Dias JM, Choi Y-J, Gong J, Bruchez MP, Liu J, Wang E (2004) Optical coding of mammalian cells using semiconductor quantum dots. Anal Biochem 327:200–208
30. Chen Q, Ma Q, Wan Y, Su X, Lin Z, Jin Q (2005) Studies on fluorescence resonance energy transfer between dyes and water-soluble quantum dots. Luminescence 20:251–255
31. Mattoussi H, Mauro JM, Goldman ER, Anderson GP, Sundar VC, Mikulec FV, Bawendi MG (2000) Self-assembly of CdSe-ZnS quantum dot bioconjugates using an engineered recombinant protein. J Am Chem Soc 122:12142–12150
32. Smith AM, Mohs AM, Nie S (2009) Tuning the optical and electronic properties of colloidal nanocrystals by lattice strain. Nat Nanotechnol 4:56–63
33. Zhang Y, Mi L, Xiong R, Wang P-N, Chen J-Y, Yang W, Wang C, Peng Q (2009) Subcellular localization of thiol-capped CdTe quantum dots in living cells. Nanoscale Res Lett 4:606–612
34. Minton AP (2001) The Influence of macromolecular crowding and macromolecular confinement on biochemical reactions in physiological media. J Biol Chem 276:10577–10580
35. Farrell CJ, Lee JM, Shin E-C, Cebrat M, Cole PA, Hayward SD (2004) Inhibition of Epstein-Barr virus-induced growth proliferation by a nuclear antigen EBNA2-TAT peptide. Proc Natl Acad Sci USA 101(13):4625–4630
36. Hotchkiss RS, McConnell KW, Bullok K, Davis CG, Chang KC, Schwulst SJ, Dunne JC, Dietz GPH, Bahr M, McDunn JE, Karl IE, Wagner TH, Cobb JP, Coopersmith CM, Piwnica-Worms D (2006) TAT-BH4 and TAT-Bcl-xL peptides protect against sepsis-induced lymphocyte apoptosis in vivo. J Immunol 176:5471–5477
37. Richard JP, Melikov K, Vives E, Ramos C, Verbeure B, Gait MJ, Chernomordik LV, Lebleu B (2003) Cell-penetrating Peptides: a reevaluation of the mechanism of cellular uptake. J Biol Chem 278(1):585–590